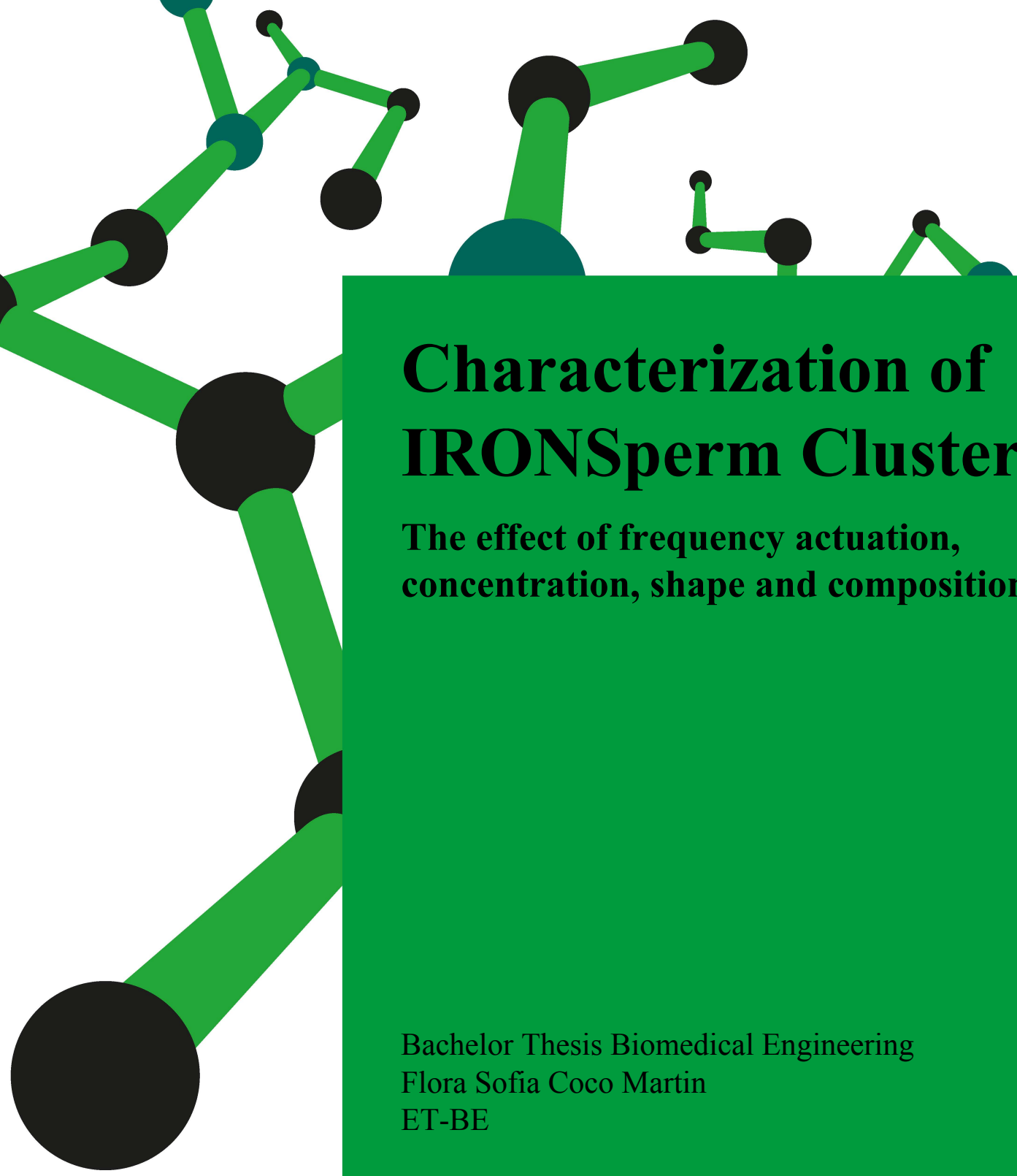

Characterization of IRONSperm Cluster

The effect of frequency actuation, concentration, shape and composition.

Bachelor Thesis Biomedical Engineering
Flora Sofia Coco Martin
ET-BE

Exam Committee:
dr. I.S.M. Khalil
dr. J. Dasdemir PhD
dr.ir. L. Alic

January 2024

SURGICAL ROBOTICS LABORATORY

UNIVERSITY OF TWENTE.

Faculty of Engineering Technology
Department of Biomechanical Engineering
Surgical Robotics Laboratory

Abstract

IRONSperm clusters are potentially considered the next-generation biohybrid microrobots for targeted drug delivery. In this research, the biohybrid microrobot IRONSperm clusters were investigated. IRONSperm consists of bull sperm cells and magnetic nanoparticles. The IRONSperm clusters were characterized considering the different concentrations of nanoparticles compared to the rolling velocity. The results showed that the optimal actuation frequency was at the cut-off frequency. Furthermore, it was observed that the IRONSperm cluster were highly inconsistent and unstable. This made the predictions of the results inconclusive. Based on this research it is recommended to have a process developed for the fabrication of IRONSperm in a homogeneous and stable manner.

Contents

1 Introduction

Currently one of the leading causes of human death is cancer, for the year 2020 more than 10 million deaths [Ferlay et al., 2020]. The most commonly applied cancer treatment for non-metastatic cancer is surgery or radiation. For metastatic cancer chemotherapy, hormone therapy or biological therapy are used. Those metastatic cancer treatments can spread via the bloodstream to reach the cancerous cells. Based on the type of tumor, the differentiation status and used treatment modality the outcome in terms of survival can be high. However, these treatments for metastatic cancer are not selective between normal tissue and tumors. Thereby they cause unwanted side effects such as the destruction of healthy cells. Even though improvements have been made to enhance selectivity in the last decade [Pérez-Herrero and Fernández-Medarde, 2015].

A more dedicated possibility to treat specifically the tumors, and not the normal tissues is by using non-invasive targeted drug delivery techniques. This technique makes it possible to deliver a drug to a specific location in the body where the tumor is located [Ashique et al., 2021]. One of the newer approaches to targeted drug delivery is based on biohybrid microrobots. Several biohybrid microrobots can guide the drug delivery system to the desired location in the body, for example using bacteria, algae or sperm cells [Lin et al., 2022]. The biohybrid microrobot used in this research is IRONSperm. IRONSperm is a sperm-templated microrobot that consists of bull sperm cells and maghemite nanoparticles. Due to the difference in charge, the sperm cells and nanoparticles have an electrostatic interaction and therefore the nanoparticles will attach to the sperm cell [Magdanz et al., 2020]. IRONSperm was found to have high flexibility and rigidity and can therefore be used for drug delivery [Magdanz et al., 2023]. To be able to use IRONSperm as a functional targeted drug delivery system it is critical to characterize its properties.

To improve the localization and locomotion of the sperm cells Middelhoek et al. [2022] made use of clusters of the IRONSperm instead of lone sperm cells. These clusters provide better visibility using imaging techniques due to the larger size of the clustered IRONSperm. In addition, the magnetic moment of the cluster is much higher compared to the single sperm cells which increases the movement of the cluster by the applied magnetic field. Besides that, the loading of drugs can be increased on a cluster [Middelhoek et al., 2022]. If the IRONSperm could be moved accurately to the target site where the tumor is located this could significantly improve the current cancer treatments and therapies.

1.1 Previous Research

In previous research by Weber [2023] on the characterization of IRONSperm, the effects of different frequencies of the rotating magnetic field on the movement of the clusters were investigated. Two sets of IRONSperm clusters were used. Both sets (A and B) consisted of one 1 mg/mL sample, one 2 mg/mL sample and one 3 mg/mL sample.

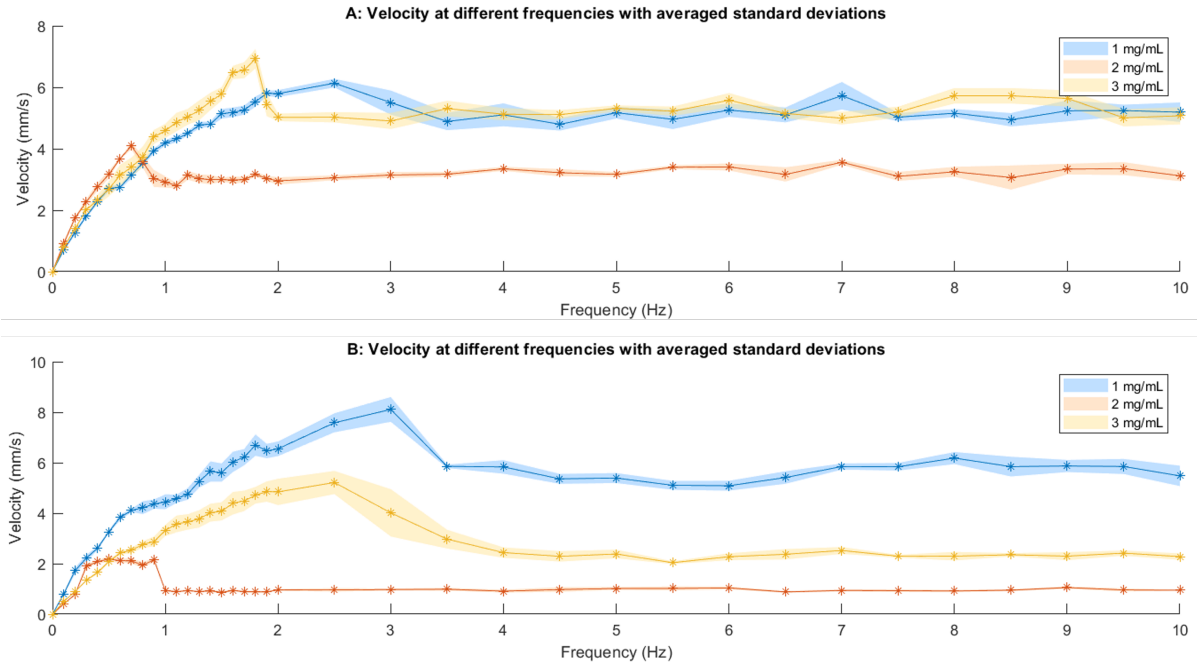

Figure 1: Sample sets A and B velocity over frequency. Each line represents a cluster with different concentrations of nanoparticles namely, 1 mg/mL, 2 mg/mL, 3 mg/mL [Weber, 2023]

.

Table 1: Concentration, volume and semi-perimeters of the approximated ellipsoidal shape of the clusters from sample sets A and B. The semi-perimeters are (a) the longest distance within the cluster, (b) the widest distance orthogonally to (a) and (c) the depth orthogonally to (a) and (b).

Measurement	**NP [mg/mL]**	**a [mm]**	**b [mm]**	**c [mm]**	**V [10^{-2} mm^3]**
A	1	4.70	2.31	1.69	7.68
	2	4.16	1.30	2.83	6.43
	3	4.72	2.18	1.68	7.27
B	1	2.85	1.77	1.16	2.45
	2	1.842	1.33	1.10	1.12
	3	2.49	1.27	0.92	1.22

Table 2: Cut-off velocities and cut-off frequencies sample set A and B.

Measurement	**NP [mg/mL]**	v **[mm/s]**	ω_0 **[Hz]**
A	1	6.13 ± 0.25	2.5
	2	4.09 ± 0.19	0.7
	3	6.93 ± 0.55	1.8
B	1	8.11 ± 0.85	3
	2	2.17 ± 0.23	0.5
	3	5.21 ± 0.80	2.5

As described by Weber [2023] no clear correlation has been found between the frequency actuation and the velocity for different concentrations of nanoparticles. As observed in Figure 1 and Table 2 there is no relation between the concentrations of nanoparticles and the velocity.

The results of Figure 1 were found using the following protocol. Each sample was placed in a perplex tube with an inner diameter of 10 mm and an outer diameter of 15 mm. The rotating permanent magnet (RPM) was placed 50 mm above the tube using the KUKA robotic arm. The FLIRBlack fly camera was placed orthogonal to the tube at a distance of 20mm. With the use of the RPM, the cluster rolled from side to side six times Weber [2023].

The data analysis from the captured videos has been performed using the Tracker Video Analysis and Modeling tool. Using the line profile the intensity was taken from each frame showing the x-position cluster over time. From this data, the velocity was calculated using Matlab.

Furthermore, Weber [2023] investigated the volume of the cluster. This has been performed with the assumption that each cluster has an ellipsoidal shape. With photographs from three viewpoints, the volume has been calculated using the three ellipsoidal axes described in Table 1. After this calculation, the velocities were normalized to the volume, but no clear outcomes were found.

1.2 Theoretical Framework

For the current research, it is proposed to use smaller IRONSperm clusters (diameter 1-3 mm). This would potentially enable the IRONSperm clusters to travel to smaller spaces within the body. Furthermore, this research aims to have a larger sample set to make the outcomes more significant. Additionally, the effects of different concentrations of nanoparticles per cluster will be examined. Because no clear outcome was found, characterization of the shape and cluster composition could give more insights into the composition of the cluster and how the shape is formed.

The method to be used to find the effect of different frequencies of the rotating magnetic field on the IRONSperm clusters with different concentrations of nanoparticles will be examined. This will be performed by placing each cluster in a tube under the rotating permanent magnet. Subsequently, RPM will rotate and the IRONSperm cluster will roll from left to right six times within the horizontally placed tube. This will be performed for all samples and the different concentrations of nanoparticles. The movement of the clusters will be recorded and examined using a tracking computer program. The data resulting from the tracking for each frequency will be analyzed, and the speed of the clusters will be calculated. The captures of both angles will provide the possibility to obtain the circularity of the IRONSperm cluster. Based on this approach it should be possible to characterize the shape and composition of the clusters.

1.3 Theoretical Background

IRONSperm clusters are gathered through self-assembly and electrostatic forces. Due to the slightly negatively charged sperm cells and the magnetic nanoparticles, the particles attract to each other. Cluster sizes can depend on the concentration of nanoparticles, and sperm cells and the time required to form a cluster. When applying the external magnetic field, the electrostatic forces between the sperm cells and the nanoparticles are increased. During the actuation of the IRONSperm cluster, it is magnetized by the external magnetic field $\mathbf{B}$. Due to the magnetic forces, the cluster wants to align with the rotation magnetic field to the preferred magnetization axis [Middelhoek et al., 2022].

The behavior of the cluster is dependent on the distribution of the nanoparticles. The fabrication is dependent on the nanoparticles, self-assembly time, and magnetic field strength. All samples are

heterogeneous and will act differently upon the applied magnetic field. The clusters are magnetized by the applied magnetic field to the magnetic moment $\mathbf{m}$, the direction of the motion is dependent on the magnetic field of the rotating magnet. The translational motion is governed by drag $\mathbf{F_d}$ and magnetic force $\mathbf{F_m}$ such that

$$\mathbf{F_d} + \mathbf{F_m} = 0 \tag{1}$$

with $\mathbf{F_d} = -f\mathbf{v}$, where f is the translational drag coefficient and $\mathbf{v}$ is the velocity. The magnetic field exerts a torque on the cluster,

$$\mathbf{T_m} = \mathbf{m} \times \mathbf{B} \tag{2}$$

This torque is balanced by the viscous drag torque

$$\mathbf{T_d} = f_r \omega \mathbf{c} \tag{3}$$

that is dependent on the rotational drag coefficient f_r and the angular velocity ωc. Considering the viscous drag coefficient is different for different cluster shapes this could effect the velocity. Furthermore, due to the contact with the wall, the rotational torque ensures a rolling locomotion. Besides the torques, Middelhoek et al. [2022] also described the relation between the moment, the magnetic field, and the applied frequency on the cut-off frequency. The cut-off frequency indicates when the cluster is unable to synchronize with the rotating permanent magnet anymore.

$$\omega_{so} = \frac{|\mathbf{m}||\mathbf{B}|}{f_r} \tag{4}$$

Since each cluster is unique in its shape, volume, and density the step-out frequency should also be dependent on this, resulting in the following formula.

$$\omega_{so} = \frac{|\mathbf{B}|^2 |n_a - n_r| V}{2\mu_0 n_a n_r f_r} \tag{5}$$

With V as the volume, μ_0 as permeability, n_a and n_r as the demagnetization factors [Middelhoek et al., 2022] .

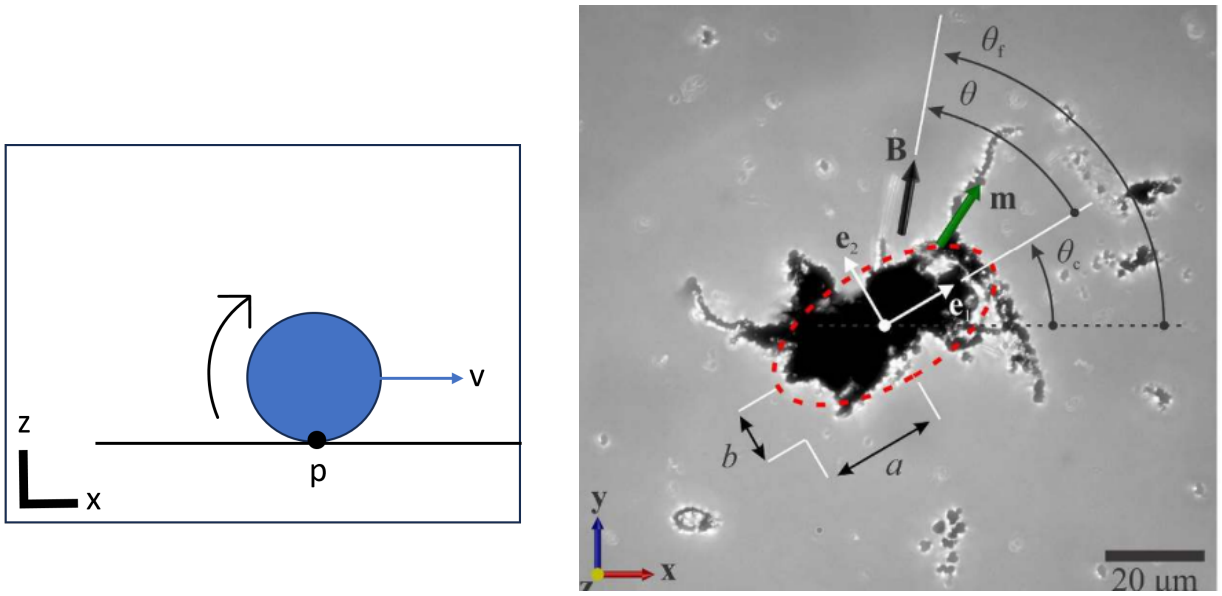

(a) (b)

Figure 2: Figure (a): A ball rolling without slipping with linear velocity v. Figure(b): The forces on the IRONSperm cluster, considering a circular shape with magnetic field B and radius r [Middelhoek et al., 2022]

.

The rolling behavior of an object is strongly dependent on its shape. A perfect example of rolling without any slipping is the rolling movement of a sphere. The forces that act on the rolling sphere are shown in Figure 2a [OpenStax, Accessed: 2023].

Furthermore, Mulder [2024] described that the shape could impact the rolling direction. When pulling the IRONSperm cluster with the RPM, due to the shape the cluster's movement was distorted and the cluster did not follow the proposed line [Mulder, 2024].

Considering a ball, it is important to know that the rolling behavior can only occur when friction occurs between the sphere and the rolling surface. To maintain the velocity of an object, the sphere needs to stay in contact with the surface, otherwise, a 'slipping' behavior will occur. The velocity of the sphere is dependent on the angular velocity and the radius of the sphere, typically when the center of rotation moves slower than the overall velocity slipping starts [Idema, 2022].

If this rolling behavior is compared to the motion of the IRONSperm cluster, it shows some similarities. If an IRONSperm cluster is not in contact with the wall it rotates but does not move in the x-direction. Like the example with the ball, if it has contact with the wall the rotational torque will cause the rolling locomotion in the x-direction. Furthermore, in the case of IRONSperm clusters, it is not dependent on the inertia but on the surface drag of the cluster, meaning that the shape is influential to the viscous drag. So for the clusters due to their unequal shape, at some point in the rolling, the cluster will lose contact as well and therefore also slip and rotate without moving in the x-direction.

Considering this, the more the shape of the cluster is like a perfect sphere the velocity should be enhanced. To test this hypothesis the clusters will be examined using photographs of six sides of the cluster and they will be compared to a perfect circle. Based on the obtained values it can be determined what the circularity of the cluster is. If the circularity is 0 it can be considered that the cluster is not circular at all. If the circularity is 1 it can be considered that the cluster is a perfect sphere. The circularity of a shape is described by

$$circularity = \frac{4\pi A}{p^2} \tag{6}$$

With A, the area and p the perimeter [Žunić and Hirota, 2008]. This could be used to make a selection between different clusters.

1.4 Research Objective

Based on the previous research on this topic there are remaining challenges to make IRONSperm the next-generation targeted drug delivery technique. Still, there are many unknowns considering the fabrication attenuation and control. Therefore, this research aims to characterize the IRONSperm clusters, by assessing:

1. The optimal frequencies to move IRONSperm clusters;
2. The velocity of the IRONSperm clusters with different concentrations of nanoparticles;
3. The shape and composition of the IRONSperm clusters.

2 Methods

2.1 Experimental method

The IRONSperm clusters were fabricated at Waterloo University as described by Magdanz et al. [2024]. In brief, a 350 μL sperm cell solution with a concentration of 2.5×10^7 cells/mL and 50/100/150 μL of Fe_3O_4 (iron oxide) nanoparticle solution of 10 mg/mL were added and then filled with distilled water to a final volume of 500 μL. The amount of nanoparticle solution resulted in different nanoparticle concentrations in the IRONSperm clusters, namely, 1 mg/mL, 2 mg/mL, and 3 mg/mL. As described in section 1.3, the clusters were assembled due to electrostatic and magnetic forces [Magdanz et al., 2024].

To determine the responsiveness of all clusters, a magnet was held close to the vials to see the response. For all responsive clusters, they were tested using the setup from Figure 3. For each cluster, the optimal distance of the rotating permanent magnet (RPM) to the cluster was determined. The cluster is placed inside the tube with an inner diameter of 10mm and an outer diameter of 15 mm in a solution of 0.9 % saline. By slowly moving the robotic arm further away from the cluster the optimal distance was determined. The RPM is set as the end effector of the KUKA robotic arm. The RPM is a cylinder magnet with NdFeB Grade-N45 and a radius of 17.5mm and 20mm thickness. Considering all clusters, the distance from the top of the tube to the RPM was set to 42mm. To capture the locomotion of the cluster the FLIR blackfly camera with a 1:1.2/6 mm lens was used. The camera was positioned perpendicular to the tube at a distance of 75mm to the side of the tube. While doing the experiments a box was put on top of the camera and the tube to maintain a white surrounding for better contrast. To determine the frequency response on the cluster the following steps were performed. For each cluster, the RPM would actuate the cluster to locomote the cluster to one side of the video frame and from that point start the recording. Then it would move from one side to the other six times. To turn the direction of the rolling cluster, the rotation direction of the RPM would be reversed.

To correlate this with the frequency the described experiment has been done for the frequencies between 0.0 Hz to 2.0 Hz in steps of 0.2 Hz, for 2.0 Hz to 5 Hz in steps of 0.5 Hz and for 5 Hz up to 10 Hz in steps of 1.0 Hz. To get the smallest error the experiments are ordered per frequency for all samples. First at 0 Hz for all samples, then 0.2 Hz for all samples and so on.

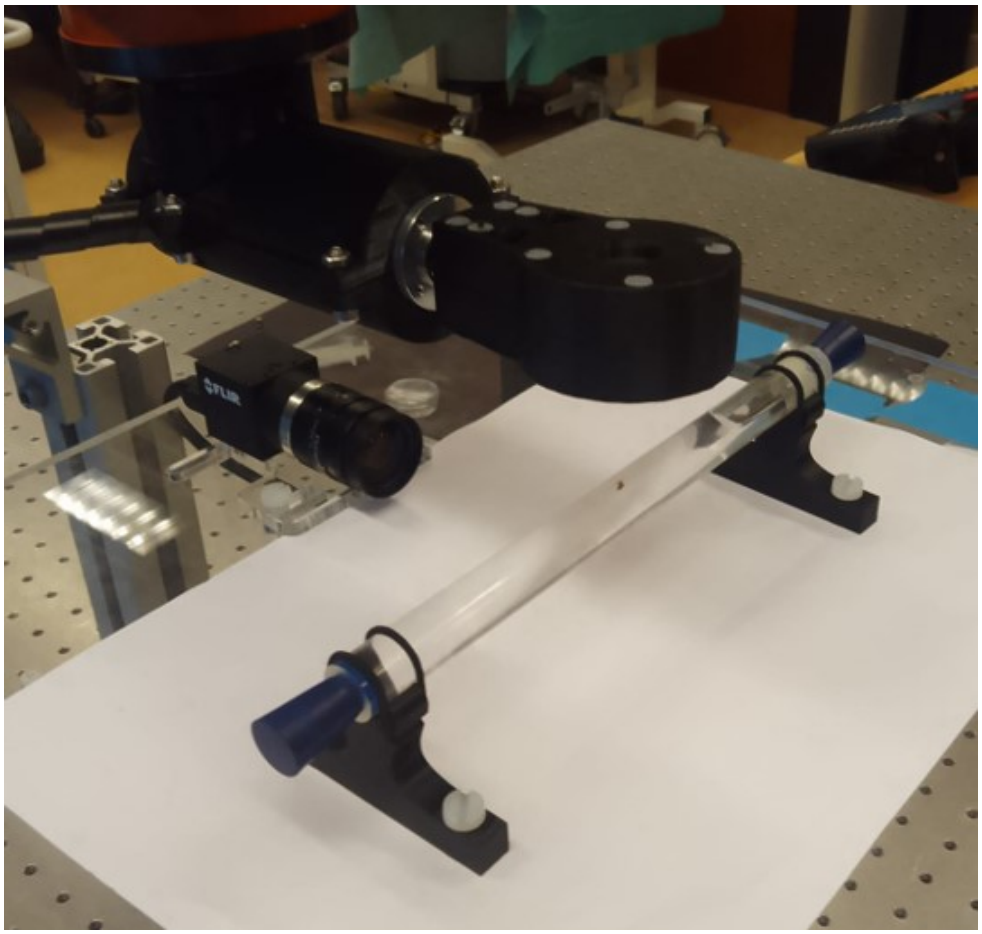

Figure 3: Experimental setup of the KUKA robotic arm and attached RPM

For assessing the shape of the cluster the clusters were photographed more closely. The camera was placed perpendicular to the perplex tube at a distance of 40mm. Again the cluster would roll from side to side and were captured using the FLIR Blackfly camera. From the videos, six video frames were taken out, showing multiple views of cluster sides.

2.2 Data analysis

The captured data has been collected using SpinView and then processed in Matlab. In Matlab, the videos are first cropped to obtain the view of interest. Then the videos were binarized, showing the cluster as a white shape and the background black. From the cluster, the centroid is determined and tracked for each frame. Using the pixel size and the actual size the displacement in the x-direction and the time were plotted. From the linear parts of the time-distance graph, the velocity was calculated. The cluster of 2 mg/mL was too small to be detected in Matlab and therefore has been processed using the Tracker Video Analysis and Modeling tool. In this program, the line profile tracked the intensity difference over a line. In this way, the data showed a peak at the point where the cluster was. This data was then inserted into Matlab, to plot the time-distance graph and calculate the velocity.

To give an insight into the effect of the shape on the velocity, the cluster images were imported to Matlab and binarized to show the outline. Then the area, and perimeter were calculated and processed in Equation 6. This has been done for all side views of the cluster and the scores are combined and averaged to represent the circularity score. From this, the circularity velocity graph is plotted.

3 Results

From the 24 IRONSperm clusters, only five were responsive, one 1 mg/mL, one 2 mg/mL and three 3 mg/mL. Those clusters will be referred to as sample set C.

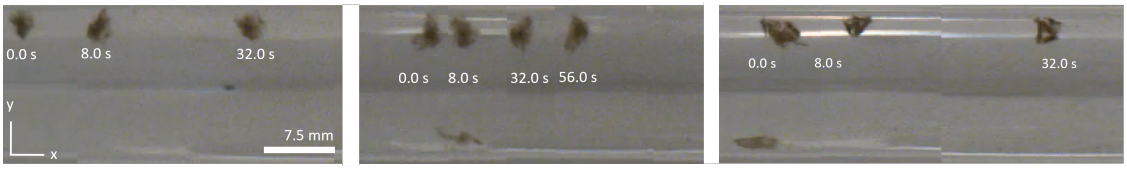

Figure 4: Rolling locomotion of three IRONSperm clusters under the actuation of the RPM with 1.6 Hz. From left to right the concentration of nanoparticles are 1 mg/mL, 2 mg/mL and 3 mg/mL

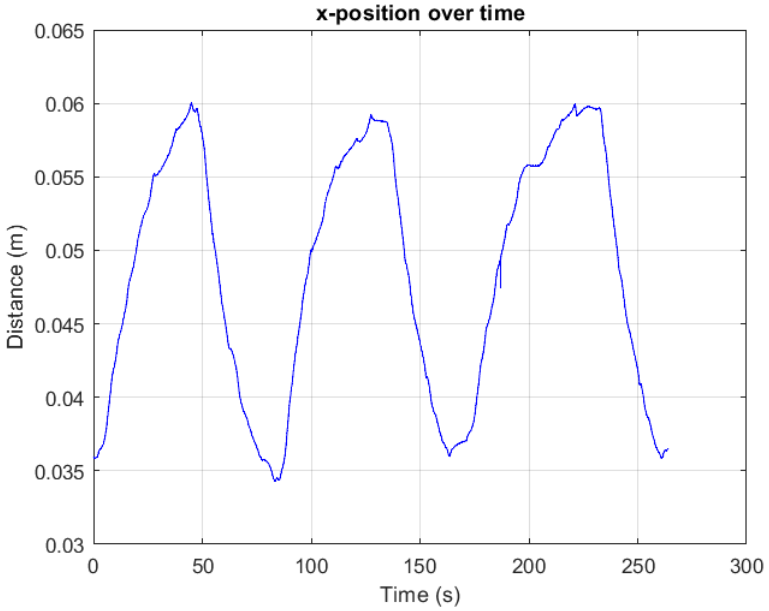

Figure 5: The x-position over time of sample set C with a nanoparticle concentration of 3 mg/mL with the actuation frequency of 1 Hz by the RPM.

From Figure 5, the velocity is obtained. The graph shows a slight increase in velocity when the cluster is moving towards the RPM with respect to moving away from the RPM.

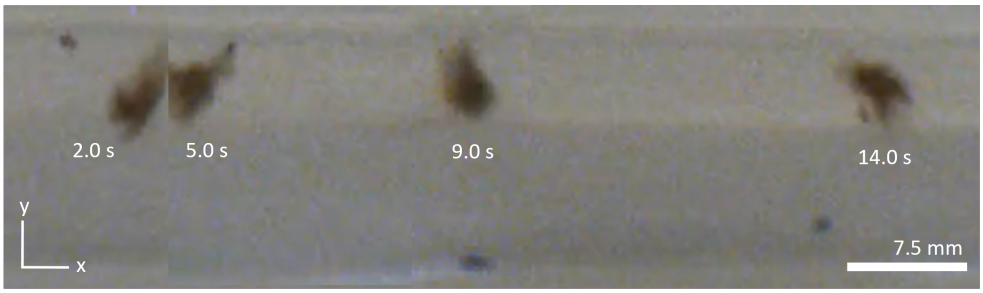

Figure 6: Rolling locomotion of cluster with 1 mg/mL concentration at 1.6 Hz actuation from sample set C. The detached cluster part attaches and increases the velocity.

As observed in Figure 6, the cluster has split up into two parts one of which is smaller and more magnetized. When the smaller part encounters the larger part, it attaches and gives the total cluster a higher velocity. Those measurements are not added to the sample set but occurred within sample set C for the 1 mg/mL and 2 mg/mL clusters.

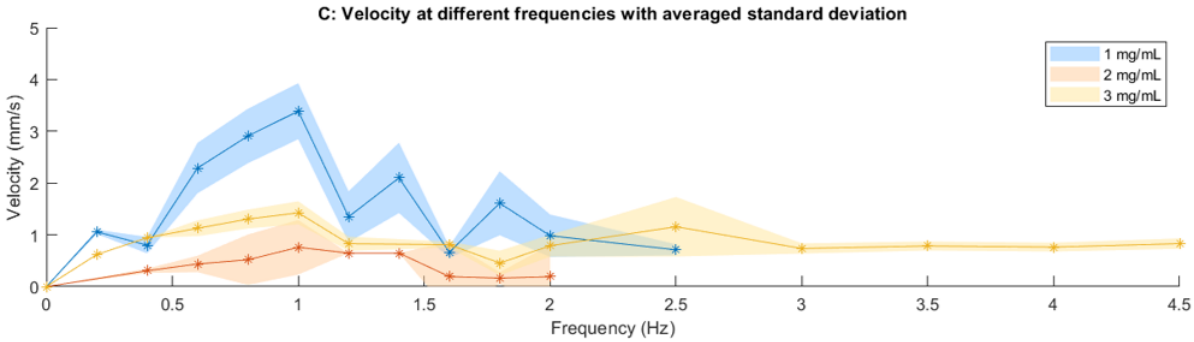

Figure 7: sample set C velocity per frequency of the RPM overall concentrations of nanoparticles.

For the concentration of 2 mg/mL and 3 mg/mL there is a linear relation between the frequency actuation and the velocity up until the cut-off frequency at 1 Hz. For the concentration of 1 mg/ mL the trend till the cut-off frequency is linear but has an offset at 0.4 Hz. During the process of actuating the cluster the 1 mg/mL and the 2mg/mL started to fall apart after reaching the cut-off frequency therefore there are no more data points collected from that point onwards. As observed in Figure 8 the rigidity and density of the clusters were lower compared to sample sets A and B. Therefore the shape consistency of sample set C was low.

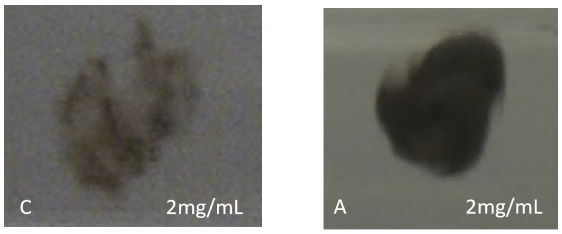

(a) (b)

Figure 8: (a) Sample set C IRONSperm cluster of concentration 1 mg/mL after all experiments. (b) Sample set A IRONSperm cluster of concentration 2 mg/mL during experiment

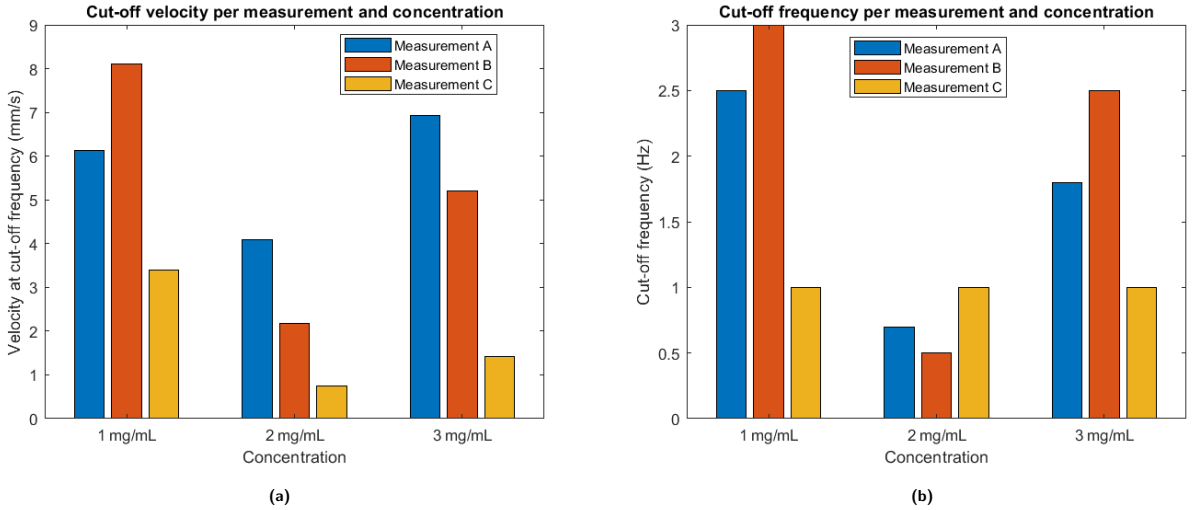

Figure 9: Graph (a) describes the cut-off velocity over all samples per concentration. Graph (b) describes the cut-off frequency over all samples per concentration.

Table 3: Cut-off velocities and cut-off frequencies sample set C

NP [mg/mL]	v **[mm/s]**	ω_0 **[Hz]**
1	3.39 ± 0.54	1.0
2	0.75 ± 0.53	1.0
3	1.425 ± 0.22	1.0

As observed from Figure 9 and Table 3 it showed that according to the Pearson correlation coefficient, the cut-off velocity and concentration correlation of sample set A, R = 0.273 (low positive correlation) [Kirch, 2008]. For sample set B, R = -0.488 (low negative correlation) and for sample set C, R = -0.716 (moderate negative correlation). Combined (the average velocity per concentration) the correlation over all measurements between the concentration and the velocity, R = -0.657 (moderate negative correlation). For the correlation between the cut-off frequency and the concentration for A: R = -0.386 (Low negative correlation), for B: R = -0.189 (no correlation) and for C: 0.0 (no correlation). Combined (the average frequency per concentration) the correlation is R = -0.315 (low negative correlation).

Table 4: Concentration, volume and semi-perimeter of the approximated ellipsoidal shape of the clusters from sample set C.

NP [mg/mL]	**a [mm]**	**b [mm]**	**c [mm]**	**V [10^{-2} mm^3]**
1	2.66	0.84	2.26	2.12
2	1.47	0.83	0.96	0.61
3	1.01	0.083	1.46	3.76

The volume of clusters in sample set C showed smaller volumes compared to sample set A but not necessarily smaller than in sample set B. Irrespective of whether the volume did not differ much the velocities were lower. In addition, the density of the clusters in sample set C was much lower compared to sample sets A and B.

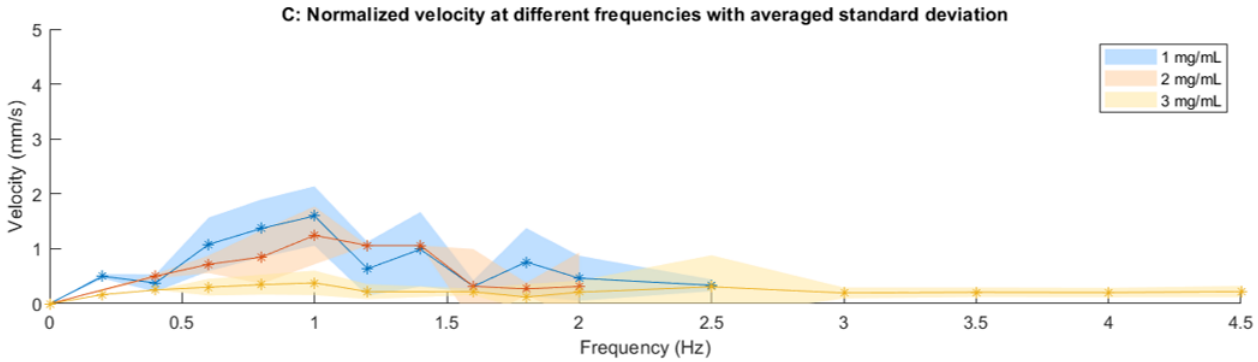

Figure 10: Velocity over frequency per concentration normalized over the volume.

Table 5: Normalized cut-off velocities and cut-off frequencies sample set C.

NP [mg/mL]	v **[mm/s]**	ω_0 **[Hz]**
1	1.59 ± 0.54	1.0
2	1.24 ± 0.53	1.0
3	0.38 ± 0.22	1.0

To obtain more comparable results the data was normalized towards the volume see, Table 4. After normalization, the results showed a negative relation between the velocity and the frequency. So for the highest achieved velocity, it correlated with the lowest concentration of nanoparticles and for the lowest velocity, it correlated with the highest concentration of nanoparticles, Figure 10 and Table 5.

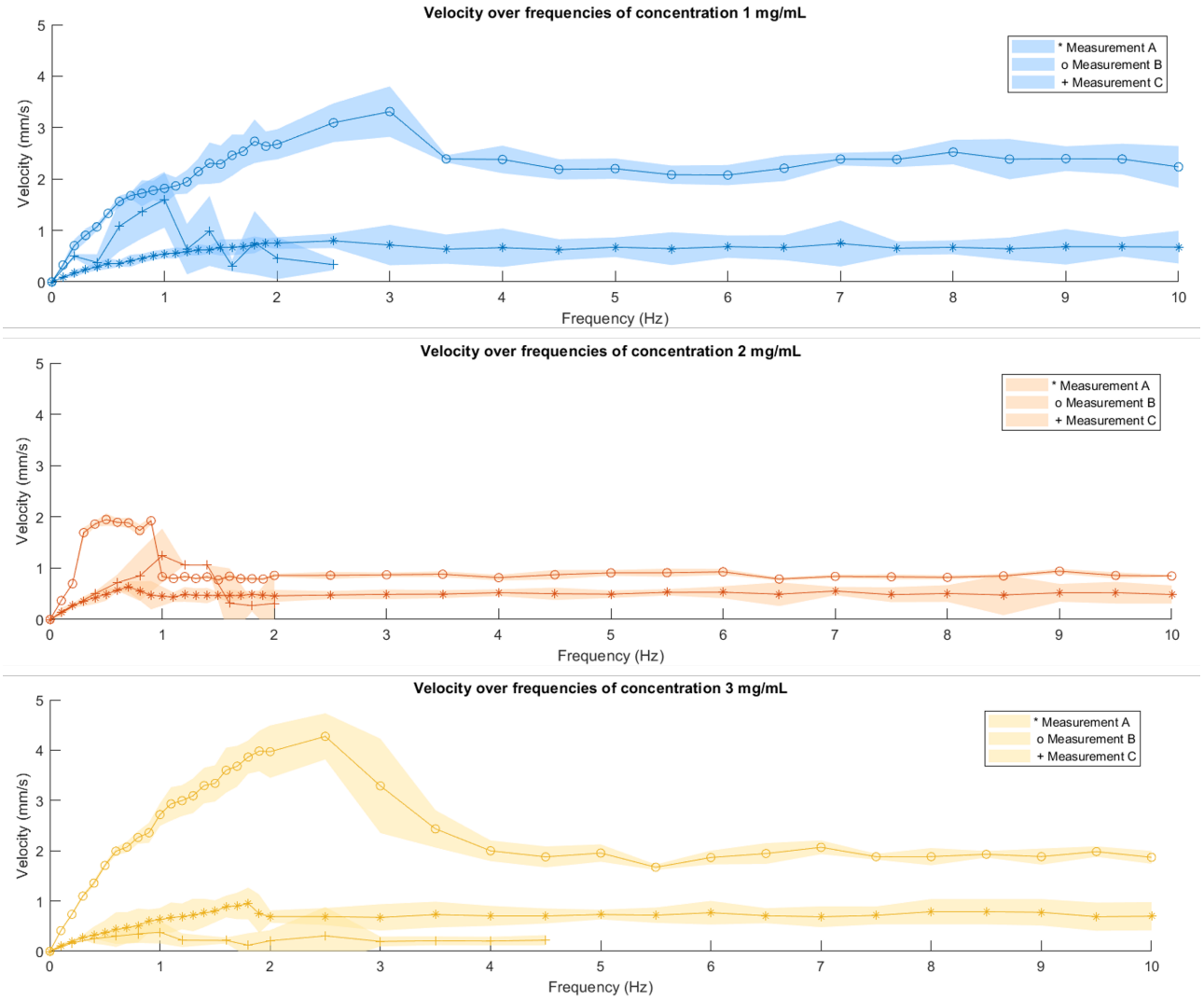

Figure 11: Velocity over frequency per concentration normalized over the volume.

As seen in Figure 11 the velocity of sample set C is slower than for sample sets A and B. For all sample sets the velocity of concentration 1 mg/mL and 3 mg/mL is higher than for concentration 2 mg/mL.

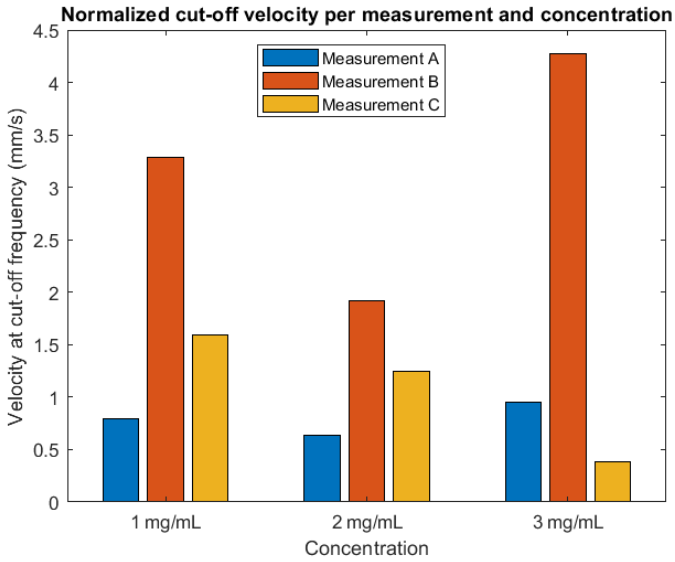

Figure 12: Velocity over frequency per concentration normalized over the volume.

After the normalization, the Pearson correlation between the concentration and the velocity was determined [Kirch, 2008]. For sample set A, R = 0.486 (low positive correlation). For sample set B, R = 0.415 (low positive correlation) and for sample set C, R = -0.972 (strong negative correlation). Combined the correlation over all measurements between the concentration and the velocity, R = 0.092 (no correlation).

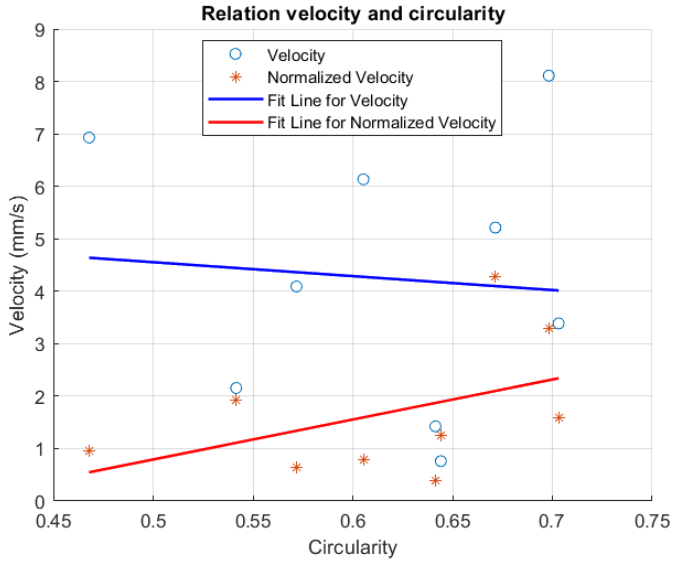

Figure 13: Velocity over frequency per concentration normalized over the volume.

Based on the picture of the clusters in Appendix A, it was observed that the clusters seemed not to be rigid and change in shape on an irregular basis. Considering this the circularity of clusters where determined and compared to their velocity. Based on the circularity and velocity for the velocity it showed R = -0.112 (No correlation) and for the normalized velocity, it showed R = 0.488 (low positive correlation).

4 Discussion

Biohybrid microrobots are potentially considered the next-generation approach for targeted drug delivery. However, to develop such a novel approach in the complex field of drug delivery many hurdles and scientific challenges need to be addressed. During this research, initial steps were taken to address some of the basic questions regarding this specific biohybrid microrobot, IRONSperm.

This study aimed to characterize the IRONSperm by assessing:

1. The optimal frequencies to move IRONSperm clusters
2. The velocity of the IRONSperm clusters with different concentrations of nanoparticles.
3. The shape and composition of the IRONSperm clusters.

To determine the answers to these unknowns several experiments were performed.

Firstly, from the 24 received IRONSperm clusters only five were responsive, one 1 mg/mL, one 2 mg/mL and three 3 mg/mL concentrations of nanoparticles. Compared to the previous research by Weber [2023] there were more responsive samples namely six, from each concentration two clusters. Therefore the robustness of the research is minimally increased. The clusters' responsiveness depends on the concentrations and distribution of the nanoparticles, the volume, magnetization and density. Due to the different responses, this could indicate there might be a slight difference between the composition of the clusters from sample sets A and B compared to sample set C. Besides that, the density and shape consistency of sample set C showed a high variation. While the shape consistency and density of sample sets A and B were more predictable. Also, Figure 6 shows this cluster instability since the cluster detaches and attaches under the actuation. Even though the fabrication of all sample sets is the same, some variation is found. Another cause for this particular behavior could be the effect of transferring the clusters in between vials and the perplex tube using a pipette. Since all measurements were taken per frequency. After each frequency, the cluster has been transferred. To get the cluster out of the pipette the pressure of the pipette acted on the cluster, possibly causing deformation. To

Secondly, there is no correlation found between the concentration of nanoparticles with respect to the velocity. However, there is a similar trend found in the research by Weber [2023]. When the frequency increases the velocity of all samples increases linearly due to their behavior to align with the RPM. At the cut-off frequency, the clusters are unable to keep up with the RPM and show a slight decrease in velocity followed by a constant speed. Compared to Weber [2023] the overall velocity of sample set C were lower. This could be explained by the lower density and responsiveness of sample set C compared to A and B.

Thirdly, the cut-off velocity (Figure 9) of sample set C showed a moderate negative correlation (R = -0.761). This is different from sample sets A and B which showed a low positive correlation (R = 0.273) and a low negative correlation (R = -0.488). Overall sample sets there is a moderate negative correlation found (R = -0.657). The cut-off frequency showed a constant value of 1 Hz for the different concentrations of nanoparticles. This is found to be the optimal frequency to move the IRONSperm cluster since it is at its highest velocity. Compared to sample sets A and B with a low negative correlation (R = -0.386) and no correlation (R = -0.189). There is no correlation found. Combined a low negative correlation (R = 0.315) was found. Due to the large variation between the cut-off velocity and the cut-off frequency over the different sample sets, it is difficult or even impossible to conclude whether there is any correlation. The variations are caused due to the volume and composition inconsistencies.

Fourthly, the volumes of the clusters differ significantly according to Table 1 and **??**. The purpose was to use a smaller cluster because for targeted drug delivery this is required. With the clusters' self-assembly process, the exact volume of the cluster is difficult to influence. Due to the differences in volume, the velocity has been normalized over the volume to reduce the effect of the volume enabling the data to be more representative. After normalization, there is a strong negative correlation (R = -0.972) found between the concentration of nanoparticles and the cut-off velocity. Compared to sample sets A and B this has not been the case. The overall correlation is not found (R = 0.092). Even though the normalization could give a better representation of the data it is based on the assumption that the cluster is ellipsoid but this is not the exact shape or volume. The variety between the sample sets is still high so clear conclusions on the correlations could not be drawn.

Lastly, there has been found a low correlation (R = 0.488) between the circularity and the normalized velocity. Considering further research it could help to make a selection between the performance of the IRONSperm.

In brief, one reoccurring problem is the inconsistency of the IRONSperm clusters. Due to their unpredictable, size, shape, magnetization, density, and composition, it is unclear what specifically caused the differences in their behavior. It is recommended for future research to develop a process to fabricate IRONSperm consistently and reliably in size, shape, magnetization, density and composition. This is not only critically required for a better characterization but, also a critical aspect of the final aim, to use the biohybrid microrobot for targeted drug delivery.

5 Conclusion

This study aimed to answer the following research objectives:

1. The optimal frequencies to move IRONSperm clusters
2. The velocity of the IRONSperm clusters with different concentrations of nanoparticles.
3. The shape and composition of the IRONSperm clusters.

The study found that the optimal velocity is at the cut-off velocity. This is the velocity where the cluster can still synchronize with the RPM. Furthermore, there is no clear correlation found between the velocity and the concentration in nanoparticles looking at all sample sets (A, B and C). This is due to the inconsistency of the formed IRONSperm clusters and their unpredictable behavior when actuated. Lastly, the shape in comparison with the circularity has been examined and showed a slight correlation. This could help to preselect IRONSperm cluster to use for treatment. This research has given insight into the current behavior of the IRONSperm cluster. In the future if the consistency of the IRONSperm clusters is examined and an effective control system is realized IRONSperm might be the next-generation targeted drug delivery technique used for cancer treatment.

References

S. Ashique, N. K. Sandhu, V. Chawla, and P. A. Chawla. Targeted drug delivery: Trends and perspectives. *Bentham Science*, 21:1–21, 2021. doi: 10.2174/1567201818666210609161301.

J. Ferlay, M. Ervik, F. Lam, M. Colombet, L. Mery, M. Piñeros, et al. Global cancer observatory: Cancer today. https://gco.iarc.fr/today, 2020. Accessed: 2023-12-18.

T. Idema. 5.8: Rolling and slipping motion - mechanics and relativity, 2022. URL https://phys.libretexts.org/@go/page/17610. Accessed: 2023-12-18.

W. Kirch, editor. *Pearson's Correlation Coefficient*, pages 1090–1091. Springer Netherlands, Dordrecht, 2008. doi: https://doi.org/10.1007/978-1-4020-5614-7_2569.

Z. Lin, T. Jiang, and J. Shang. The emerging technology of biohybrid micro-robots: a review. *Biodesign and Manufacturing*, 5:107–132, 2022. doi: https://doi.org/10.1007/s42242-021-00135-6.

V. Magdanz, I. S. M. Khalil, J. Simmchen, G. P. Furtado, S. Mohanty, J. Gebauer, H. Xu, A. Klingner, A. Aziz, M. Medina-Sánchez, O. G. Schmidt, and S. Misra. Ironsperm: Sperm-templated soft magnetic microrobots. *Science Advances*, 6(28):eaba5855, 2020. doi: 10.1126/sciadv.aba5855.

V. Magdanz, A. Klingner, L. Abelmann, and I. Khalil. Ironsperm swimming by rigid-body rotation versus transverse bending waves influenced by cell membrane charge. *Journal of Micro-Bio Robotics*, 18, 2023. doi: https://doi.org/10.1007/s12213-023-00158-5.

V. Magdanz, Y. Pervez, M. LaBrash-White, M. Bloxs, S. Mohsenkani, M. Gorbet, N. Bouzari, H. Shahsavan, L.-J. W. Ligtenberg, L. Weber, H. R. Liefers, M. Warle, and I. S. M. Khalil. Sperm cell empowerment: X-ray-guided magnetic fields for enhanced actuation, localization of cytocompatible biohybrid microrobots. 2024.

K. I. Middelhoek, V. Magdanz, L. Abelmann, and I. S. Khalil. Drug-loaded ironsperm clusters: Modeling, wireless actuation, and ultrasound imaging. *Biomedical Materials*, 17(6):065001, 2022. doi: 10.1088/1748-605x/ac8b4b.

I. Mulder. Localization and 2d locomotion control of ironsperm clusters in vitro. *Manuscript in preparation*, 23:1–23, 2024. University of Twente, Enschede.

OpenStax. 11.1 rolling motion, Accessed: 2023. URL https://pressbooks.online.ucf.edu/osuniversityphysics/chapter/11-1-rolling-motion/. Accessed: 2023-12-18.

E. Pérez-Herrero and A. Fernández-Medarde. Advanced targeted therapies in cancer: Drug nanocarriers, the future of chemotherapy. *European Journal of Pharmaceutics and Biopharmaceutics*, 93: 52–79, 2015. doi: https://doi.org/10.1016/j.ejpb.2015.03.018.

L. Weber. Frequency actuation of different concentrations ironsperm in in vitro situation. 23:1–23, 2023. Univerity of Twente, Enschede, Unpublished.

J. Žunić and K. Hirota. Measuring shape circularity. In J. Ruiz-Shulcloper and W. G. Kropatsch, editors, *Progress in Pattern Recognition, Image Analysis and Applications*, pages 94–101, Berlin, Heidelberg, 2008. Springer Berlin Heidelberg. doi: https://doi.org/10.1007/978-3-540-85920-8_12.

Appendices

A Cluster photographs sample set C

Figure 14: IRONSperm cluster concentration 1 mg/mL

Figure 15: IRONSperm cluster concentration 2 mg/mL

Figure 16: IRONSperm cluster concentration 3 mg/mL

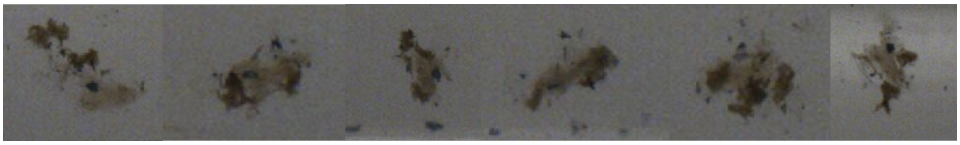

Figure 17: IRONSperm cluster concentration 3 mg/mL

Figure 18: IRONSperm cluster concentration 3 mg/mL